

# Ge/Si Hetero-Junction Hetero-Gate PNP TFET with Hetero-Dielectric BOX to Improve $I_{ON}/I_{OFF}$

S. M. Turkane<sup>1,2\*</sup>, G. K. Kharate<sup>1</sup> and A. K. Kureshi<sup>3</sup>

<sup>1</sup>Matoshri College of Engineering and Research Centre, Savitribai Phule Pune University, Nashik – 422105, Maharashtra, India; satish\_turkane@yahoo.co.in, gkkharate@rediffmail.com

<sup>2</sup>Pravara Rural Engineering College, Ahmednagar, Savitribai Phule Pune University, Loni – 413736, Maharashtra, India

<sup>3</sup>Vishwabharti Academy's College of Engineering, Savitribai Phule Pune University, Ahmednagar - 414201, Maharashtra, India; akkureshi@rediffmail.com

## Abstract

**Objective:** PNP TFET is a semiconductor device in which the gate controls the source to channel tunneling current through modulation of band-to-band tunneling. Silicon film thickness is also optimized to remove the kink effect. **Methods/Statistical Analysis:** As the Silicon device technology as downsized to nanometers, it experiences certain issues like short channel effects, low  $I_{ON}/I_{OFF}$  and low Sub-threshold Slope. The hetero-gate dielectric structure is designed with the addition of a hetero-dielectric Buried Oxide (BOX) on the doped substrate for reduction of ambipolar current and improvement of tunneling current at drain and source side respectively. The hetero-dielectric BOX has  $SiO_2$  dielectric below source/channel regions and  $HfO_2$  below the drain region. **Findings:** The proposed device type is of Ge/Si Hetero-junction hetero-gate dielectric with hetero-dielectric BOX PNP Tunnel FET with low bandgap material at source region increases the tunneling probability and hence improves  $I_{ON}$ . Various combinations of the simulation where executed with reference to channel, source, drain and N pocket doping for getting the optimized results for Id-Vg characteristics. The entire simulations were done in licensed Cogenda TCAD version 1.7.4 software. The hetero-gate dielectric improves the  $I_{ON}$  and suppresses the ambipolar current. Also DIBN effect gets reduced because drain current is not varied with changes in  $V_{ds}(V)$  values with respect to  $V_{gs}(V)$  values. With the proposed device we obtained the performance parameters as  $I_{ON}=1.24mA/\mu m$ ,  $SS=44.66mV/dec$  and  $I_{ON}/I_{OFF}=3.47\times 10^{12}$ . **Applications/Improvements:** Modeled PNP TFET had resulted in improved performance in-terms of  $I_{ON}/I_{OFF}$  ratio, using low band gap material and hence is best alternative over the conventional CMOS devices for the low power and moderate speed applications of FPGA.

**Keywords:** Ambipolar Behavior, Band-to-Band Tunneling, Hetero-Dielectric BOX, Hetero-Gate, Power Delay Product (PDP), Sub-Threshold Slope, Tunnel FET

## 1. Introduction

As Metal-Oxide Semiconductor field effect transistor (MOSFET) scaled down, it showed the limiting factors based on short channel effects, Sub-threshold slope  $>60mV/decade$ . Now a day's lot of work has been done on band to band tunneling principle based Tunnel Field Effect Transistor (TFET) devices<sup>1-3</sup>. The Tunnel FET have p-i-n

structure which works by means of gate modulated tunneling, in any case it has one of the significant disadvantage of not having sharp tunneling near the source bending, due to which its  $I_{ON}$  gets reduced and which is not compatible with the ITRS requirement. So the obtained SS is higher than  $60mV/decade$ <sup>4,5</sup>. The p-i-n structure have large tunneling width, due to that voltage drop occurs the tunneling junction reduces the  $I_{ON}$ . Generally conventional TFET have

\*Author for correspondence

10 $\mu$ A  $I_{ON}$  which is half of ITRS requirement<sup>6</sup>. Various TFET types has been proposed in last two decades, starting from the Surface Tunnel Transistor, p-i-n based TFET, Feedback TFET, Vertical TFET, Junction less TFET, DG-TFET, p-n-i-n TFET Raised Buried Oxide Tunnel FET, Hetero-junction TFET, and Doping less TFET<sup>7</sup>. The idea of PNP TFET<sup>4</sup> has been proposed as an alternative for getting enhanced SS and  $I_{ON}/I_{OFF}$ . Hetero-gate dielectric PNP TFET is presented in<sup>8</sup>.

The homojunction tunnel FET has some shortcomings like<sup>7,9-11</sup> minimum  $I_{ON}$ , ambipolar behavior, high  $I_{OFF}$  and maximum SS. As we use small band gap materials, they improve  $I_{ON}$  but at the same time  $I_{OFF}$  also gets increased<sup>12-14</sup>, this happens as the TFET shows ambipolar behavior. In ambipolar behavior as we apply the negative gate bias, conduction occur at the drain/channel junction. This ambipolar behavior of TFET can be suppressed by making asymmetric structure with the help of different doping for the drain and the source region including different gate oxide materials with high k dielectric material near source region. Besides utilizing materials with smaller band gaps, hetero-junction devices could also be adopted. Using of small band gap material, the on-state current could be improved<sup>15</sup>. Channel and drain regions are made with materials having larger band gap, so that drain side tunneling leakage could be suppressed.

In this paper we propose a Ge/Si Heterojunction hetero-dielectric PNP Tunnel FET which adds a hetero-dielectric BOX on the highly doped ground plane. The device is designed and simulated using licensed Cogenda TCAD software version 1.7.4. The structure surpasses the Drain – Induced Barrier Narrowing (DIBN) effect, which had been predominant in the previous designed PNP structure.

The paper is sorted as follows: A brief presentation concerning Tunnel FET device is given in section-I. Section II portrays the device structure and its simulation. In section III, the electrical characteristic of proposed device has been analyzed. Section IV displays the outcomes and discussion about the proposed Ge/Si heterostructure hetero-gate dielectric with hetero-dielectric BOX PNP Tunnel FET. At last, section V specifies the conclusion.

## 2. Device Structure and Simulation

Rather than utilizing p+ source as a part of an ordinary TFET, a tunneling junction is framed between the

p+ area and a completely depleted thin n layer under the gate which decreases the tunneling width and makes nearby band bowing and in this manner a steep subthreshold slope is gotten. This n pocket enhances the tunneling by accomplishing steep subthreshold conduct and in the meantime gives high  $I_{ON}$  when contrasted with ordinary PNP TFET utilizing Gate oxide made of HfO<sub>2</sub> (k=25) and SiO<sub>2</sub> (k=3.9)<sup>17</sup>. An option way to deal with totally wipe out the ambipolar conduction in TFETs by utilizing a hetero-dielectric BOX over a vigorously doped (P+) substrate of a N-channel PNP TFET. The proposed device design encourages the depletion of the drain area at the channel-drain interface expanding the tunneling obstruction width on the drain side bringing about the suppression of the ambipolar conduction<sup>16</sup>.

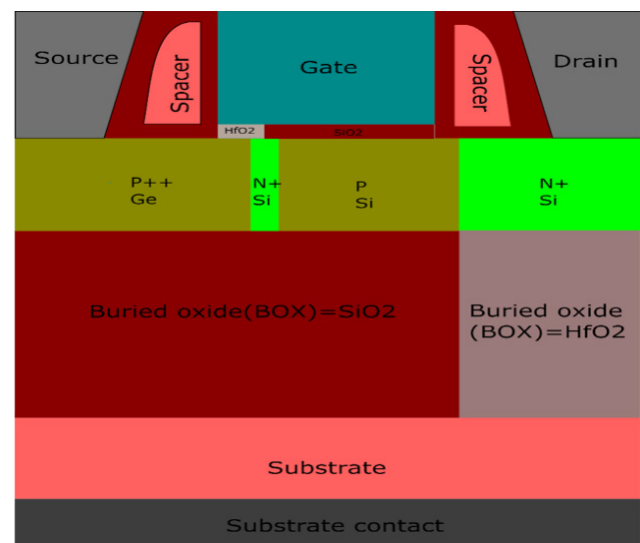


Figure 1. Structure of PNP TFET.

The Ge/Si Heterojunction hetero-gate dielectric with hetero-dielectric BOX PNP TFET structure is shown in Figure 1 Technology Computer Aided Design (TCAD) is an intense tool for 2D/3D simulation of devices. A device design can be optimized for decreasing the design costs, enhancing the device design efficiency and getting the better device and the technology designs. The simulation is helpful in predicting the electrical characteristics of devices. We have used a Kane Band-to-Band Tunneling model in which value of two parameters of Kane's model are A.BTBT =  $3.9e+22eV^{(-1/2)}cm^{-1}s^{-1}V^{-2}$  and B.BTBT =  $2.25e+07 Vcm^{-1}eV^{(-2/3)}$ . Also a mobility model like Lombardi mobility model is used.

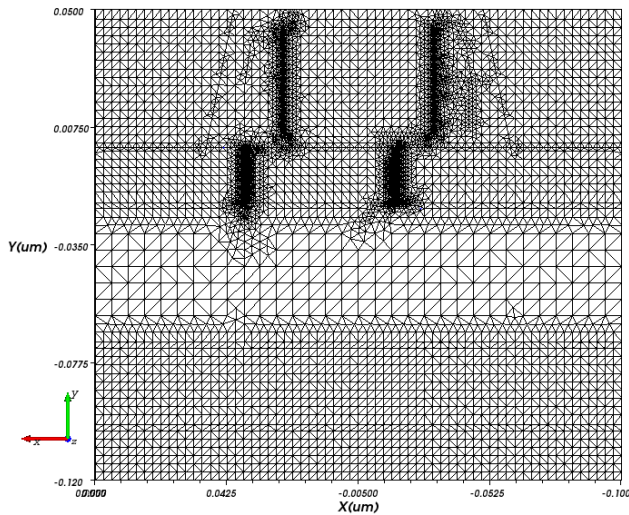


Figure 2. Mesh structure of the PNP Tunnel FET.

A meshing is applied to the whole device to create the calculation points where the semiconductor equations are applied. Figure 2 shows a mesh structure of the simulated PNP Tunnel FET. We can visualize that meshing is dense near the gate oxide/source/channel tunnel junction, where actual tunneling in TFET occurs so that accurate values of current and voltages can be predicted. When meshing is applied, the TCAD simulation software automatically predicts the junction points and finer mesh is applied to the region. Before we finalize our device parameters, we simulated the device and varied various parameters to analyze which device gives the best performance. Simulations are done at  $V_{ds} = 1.2V$  and  $V_{gs}$  is varied from 0 to 2.5V.

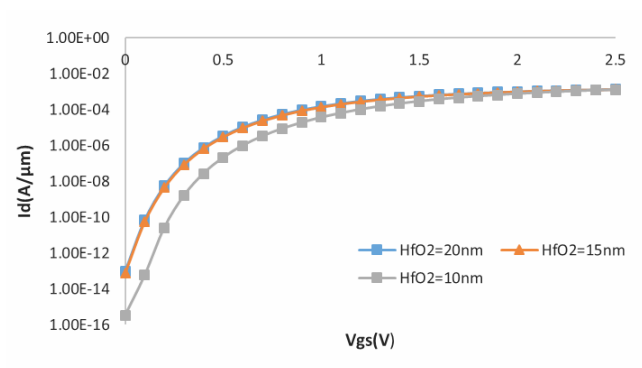


Figure 3. Id-Vg characteristics of  $HfO_2$  length variations.

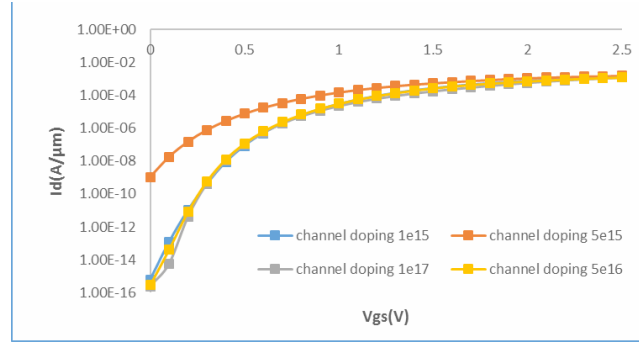


Figure 4. Channel doping variations.

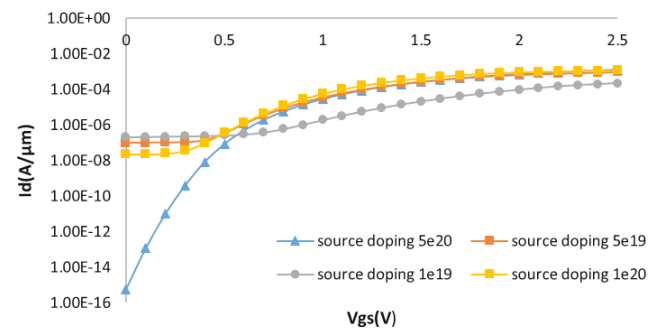


Figure 5. Source doping variations.

In the proposed device we have used two dielectrics for gate oxide namely: High-k  $HfO_2$  and Low-k  $SiO_2$  hetero-dielectric. The Plot of  $I_d$ - $V_{gs}$  characteristics for various  $HfO_2$  lengths are shown in Figure 3. Among them at 10nm we get higher  $I_{ON}$ . To ponder the impact of channel doping on device performance, we have varied the channel doping, keeping source and drain doping to  $5e+20$  atoms/cm<sup>3</sup> and  $5e+18$  atoms/cm<sup>3</sup> respectively. The proposed device is N- type Tunnel FET, in which channel region is n type doped. We varied the  $N_d$  concentration from  $1e+15$ ,  $5e+15$ ,  $1e+16$ ,  $5e+16$  and  $1e+17$  atoms/cm<sup>3</sup>. Drain current values for channel doping with  $5e+15$ atoms/cm<sup>3</sup> are better among them. There is not much difference in the  $I_d$ - $V_{gs}$  characteristics for these values as indicated in Figure 4. At  $5e+20$ atoms/cm<sup>3</sup> have better drain current for source doping as shown in Figure 5. Also n packet doping's varying with  $1e+19$ ,  $5e+18$ ,  $5e+19$  and  $1e+20$  atoms/cm<sup>3</sup>. Among them  $1e+19$  shows better  $I_{ON}$  as shown in Figure 6. The alternative variations in work function for 4.17, 4.33,

4.7 and 4.5eV where analyzed; 4.5eV shows steeper performance as indicated in Figure 7. When we change the position of the N packet which is extra layer in PNPN, it changes its  $I_d$ - $V_g$  characteristics and it shows superior performance under half of  $HfO_2$  and half of  $SiO_2$  as drawn in Figure 8. The simulated device parameters are listed in Table 1 which indicates region materials, contact materials, region thickness/length and doping concentrations of the regions. Gate material is of NpolySi.

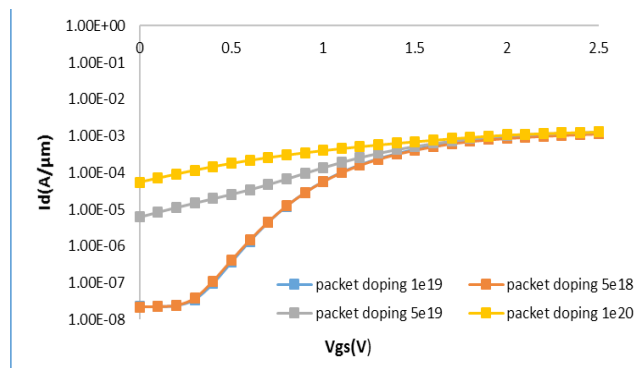


Figure 6. N packet doping variations.

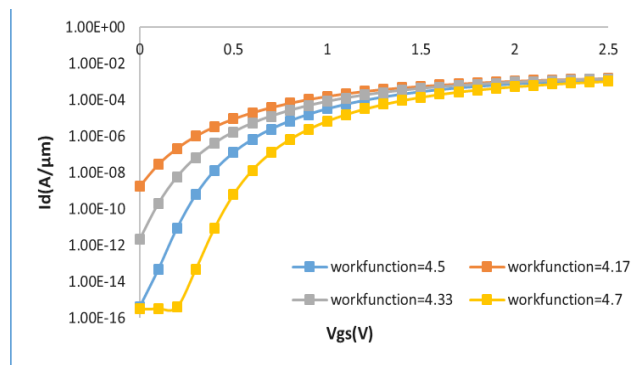


Figure 7. Work function variations.

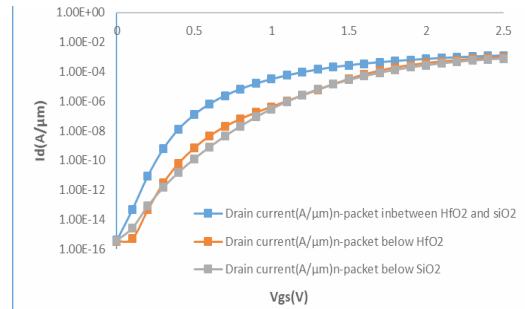


Figure 8. N packet position variations.

In the proposed device we have used two dielectrics for gate oxide namely: High-k  $HfO_2$  and Low-k  $SiO_2$  hetero-dielectric. The Plot of  $I_d$ - $V_g$  characteristic for various  $HfO_2$  lengths is shown in Figure 3. Among them at 10nm we get higher  $I_{ON}$ . To ponder the impact of channel doping on device performance, we have varied the channel doping, keeping source and drain doping to  $5e+20$  atoms/cm<sup>3</sup> and  $5e+18$  atoms/cm<sup>3</sup> respectively. The proposed device is N-type Tunnel FET, in which channel region is n type doped. We varied the  $N_d$  concentration from  $1e+15$ ,  $5e+15$ ,  $1e+16$ ,  $5e+16$  and  $1e+17$  atoms/cm<sup>3</sup>. Drain current values for channel doping with  $5e+15$  atoms/cm<sup>3</sup> are better among them. There is not much difference in the  $I_d$ - $V_g$  characteristics for these values as indicated in Figure 4. At  $5e+20$  atoms/cm<sup>3</sup> have better drain current for source doping as shown in Figure 5. Also n packet doping's vary with  $1e+19$ ,  $5e+18$ ,  $5e+19$  and  $1e+20$  atoms/cm<sup>3</sup>. Among them  $1e+19$  shows better  $I_{ON}$  as shown in Figure 6. The alternative variations in work function for 4.17, 4.33, 4.7 and 4.5eV where analyzed; 4.5eV shows steeper performance as indicated in Figure 7. When we change the position of the N packet which is extra layer in PNPN, it changes its  $I_d$ - $V_g$  characteristics and it shows superior performance under half of  $HfO_2$  and half of  $SiO_2$  as drawn in Figure 8. The simulated device parameters are listed in Table 1 which indicates region materials, contact

Table 1. Design parameters of the device

Region	Contact material	Material	Thickness/ Length	Doping (Atoms/cm <sup>3</sup> )
Source	Aluminium (Al)	Ge	50nm	$N_A$ (P++ type) $5 \times 10^{20}$
Drain	Aluminium (Al)	Si	50nm	$N_D$ (N+ type) $5 \times 10^{18}$
Channel	–	Si	50nm	$N_D$ (N type) $5 \times 10^{15}$
N pocket	–	Si(4nm)	20nm	$N_D$ (P type) $1 \times 10^{19}$
Substrate	Aluminium (Al)	Si	30nm	$N_A$ (P type) $1 \times 10^{17}$
Buried Oxide	–	$SiO_2$ (136nm) + $HfO_2$ (54nm)	50nm	–
Gate Oxide	–	$HfO_2$ (10nm) + $SiO_2$ (40nm)	4nm	–
Spacer	–	Nitride	20nm	–

materials, region thickness/length and doping concentrations of the regions. Gate material is of NpolySi.

### 3. Electrical Characteristics of Proposed Device

The choice of source/channel materials with the reduced (effective) band gap is important for increasing tunneling current with suppressing OFF current. By utilizing materials with smaller band gaps, the on-state current of a tunneling FET could be greatly improved. The flow of electric current is from source region to channel region and then from channel region to drain region whereas the flow of hole current is from drain region to channel region and from channel region to source region which is seen in Figure 9 and Figure 10 respectively. Figure 11 shows that by varying  $V_{ds}$  from 0V to 2.4V; the plot of  $I_d$  vs  $V_{gs}$  are analyzed. These values predict that, for different values of  $V_{ds}$ ,  $I_d$  value varies in a small fraction. It means that the proposed device doesn't show any drain induced barrier narrowing (DIBN) effect<sup>17</sup>.

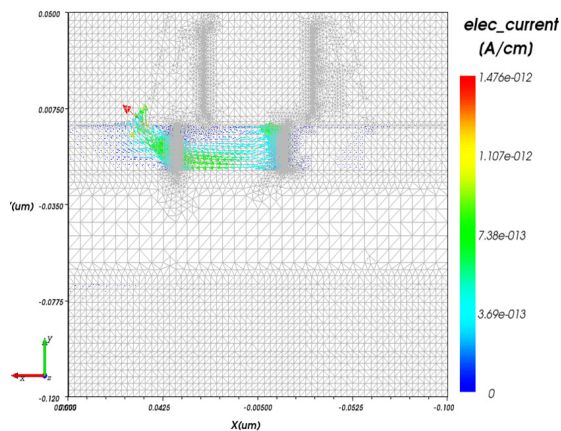


Figure 9. Electric current.

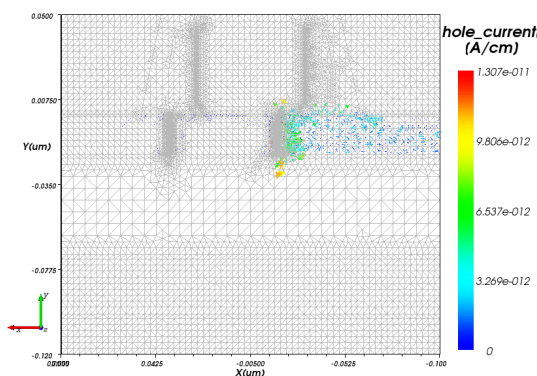


Figure 10. Hole current.

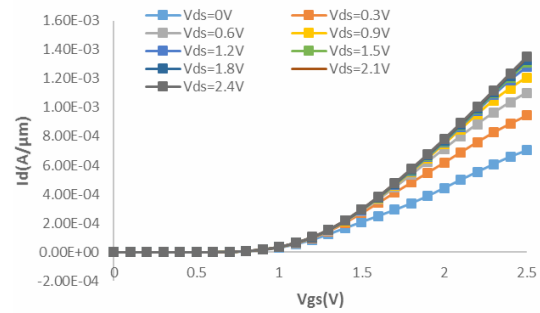


Figure 11.  $I_d$ - $V_g$  characteristics.

When PNP TFET is in OFF-state i.e.  $V_{gs} = 0V$ ; TFET is reverse biased which ends up in larger tunneling barrier width. A High-k  $HfO_2$  dielectric oxide is used near source/channel junction due to which valance band of channel near source end will be increased. This reduces the tunneling probability and thus we get lowest OFF-state current as appeared in Figure 12. Once TFET is in ON state i.e.  $V_{gs} = 2.5V$ , electrons begin tunneling from valance band of P++ source to the conduction band of the N channel then towards the conduction band of the N+ drain region<sup>18</sup> as shown in Figure 13. In Figure 14 potential distribution is shown at  $V_{dd}=0.6V$ ; when  $V_{gs}=0V$  then potential distribution is in linear manner and when  $V_{gs}=2.5V$  it increases in appropriate proportion.

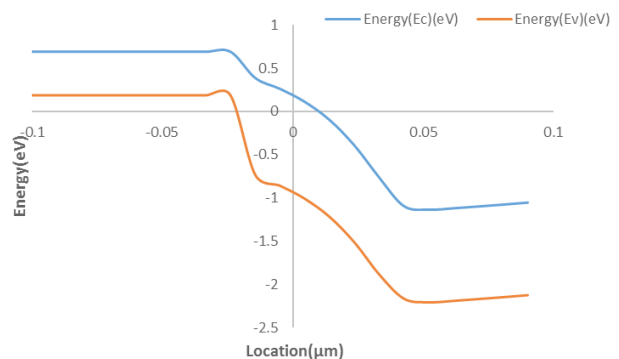


Figure 12. Energy band diagram at  $V_{gs}=0V$ .

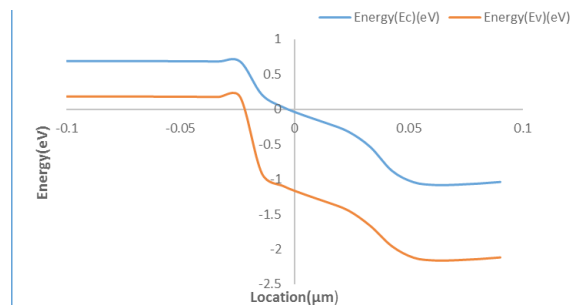
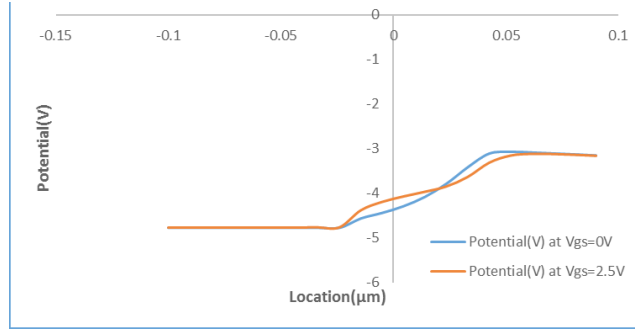


Figure 13. Energy band diagram at  $V_{gs}=2.5V$ .



**Figure 14.** Potentials distribution at Vdd=0.6V.

## 4. Results and Findings

From the electrical characteristics, we studied and analyzed the performance of the device. We extracted  $I_{ON}$ ,  $I_{OFF}$ , Sub-threshold slope, switching delay, power dissipation and PDP from simulated data at Vdd=0.6V,  $I_{ON}=9.62 \times 10^{-7} \text{ A}/\mu\text{m}$  and  $C_{g,avg}=1 \times 10^{-15} \text{ F}$ .

### 4.1 Subthreshold Slope/Swing (SS)

The sub-threshold swing (SS) is vital property of TFET: smaller the SS, the better is the dynamic performance. Subthreshold Swing/Slope can be described as Gate Voltage required to change drain to Source current by one decade. It can be determined as the inverse of slope of the log  $I_d$  vs  $V_{gs}$  curve, in the subthreshold exponential region<sup>19</sup>.

$$SS = \frac{\partial V_{gs}}{\partial (\log I_d)} \quad (1)$$

The switching speed of a device is determined by SS<sup>20</sup>.

### 4.2 Transconductance

It is defined as the adjustment in the drain current divided by the little change in the gate-to-source voltage with a consistent drain-to-source voltage and it is measured in Siemens.

$$g_m = \frac{\partial I_d}{\partial V_g} \quad (2)$$

### 4.3 Switching Delay

Switching delay is given by<sup>21</sup>.

$$\tau = \frac{C_{g,avg} V_{dd}}{I_{ON}} \quad (3)$$

$C_{g,avg}$  is average capacitance across the gate bias range.

### 4.4 Dynamic Power Dissipation

$$P_{dynamic} = C_{g,avg} V_{dd}^2 f \quad (4)$$

### 4.5 Power Delay Product

Represents Power-Performance trade-off at provided operation frequency and is given by<sup>21</sup>.

$$PDP = C_{g,avg} V_{dd}^2 f \times t_{delay} \quad (5)$$

The electrical parameters that we have considered in this paper are the following: the ON-current and the sub-threshold swing. The ON-current is defined as the drain current at a gate voltage of 0.6V. The threshold voltage is defined as the gate voltage when the drain current reaches  $1 \times 10^{-7} \text{ A}/\mu\text{m}$ . For  $V_{ds}=0.6\text{V}$ ;  $I_{OFF}=3.17 \times 10^{-16} \text{ A}/\mu\text{m}$  at  $V_{gs}=0\text{V}$  and  $I_{ON}=1.24 \text{ mA}/\mu\text{m}$  at  $V_{gs}=2.5\text{V}$ .

Results are listed in Table 2.

**Table 2.** Simulated results

Parameters	Proposed TFET Device
$I_{ON}(\text{mA}/\mu\text{m})$	1.24
$I_{OFF}(\text{fA}/\mu\text{m})$	0.317
$I_{ON}/I_{OFF} (\times 1012)$	3.47
Subthreshold Slope(mv/dec)	44.66
Transconductance( $\times 10^{-6} \text{ S}$ )	7.84
Switching delay (psec)	623.7
Power dissipation (pWatt)	0.36
PDP ( $\times 10^{-22} \text{ J}$ ) at $V_{ds} = 0.6\text{V}$	2.24

## 5. Conclusion

The Ge/Si Heterojunction hetero-gate dielectric with hetero-dielectric BOX PNP Tunnel FET with low band-gap material at source region increases the tunneling probability and hence improves  $I_{ON}$ . With the different variations of channel, source, drain and N pocket doping, we selected best value from Id-Vg characteristics. Also we had varied the work function for exploring the possibilities of improvement of  $I_{ON}$  and reduction of  $I_{OFF}$ . Hetero gate dielectric improves the  $I_{ON}$  and suppress the ambipolar current. Also DIBN effect gets reduced because drain current is not varied with changes in  $V_{ds}(\text{V})$  values with respect to  $V_{gs}(\text{V})$  values. Heterodielectric Buried Oxide (BOX) layer reduces the parasitic capacitance and reduces

the leakage currents and also suppress the ambipolar behavior. We obtained  $I_{ON}/I_{OFF}=3.47\times 10^{12}$ ,  $SS=44.66\text{mV/dec}$  which is greater than [17]. From this study, we conclude that PNP TFET with low bandgap materials and with the combinations of hetero-dielectric is the promising key alternative for high speed low power FPGA applications. In future, with the help of low band gap materials like SiGe/Si with varied concentration PNP TFET can be designed.

## 6. References

- Appenzeller J, Lin YM, Conch J, Avouris P. Band-to-band tunneling in carbon Nanotube fiel-effect transistors. 2004; 93(19): 196805-1–196805-4.
- Bhuwalka K, Sedlmaier S, Ludsteck A, Tolksdorf C, Schulze J, Eisele I. Vertical tunnel field effect transistor, IEEE Transactions on Electron Devices. 2004 Feb; 51(2): 279–82. Crossref
- Reddick W, Amartunga G. Silicon surface tunnel transistor. 1995 May; 67(4): 494–6.
- Girish NV, Jhaveri R, Woo CS. The Tunnel Source (PNPN) n-MOSFET Novel High Performance Transistor. IEEE Transactions on Electron Devices. 2008 April; 55(4): 1013–9.
- Gopalakrishnan k, Griffin p, Plummer J. I-MOS a novel semiconductor device with a subthreshold slope lower than  $kT/q$  in IEDM Technical Digest. 2002; 289–92.
- Semiconductor Industry Association (SIA), International Technology Roadmap for Semiconductors (ITRS), 2009. Available from: Crossref online accessed. 02-05-2016.
- Turkane SM, Kureshi AK. Review of Tunnel Field Effect Transistor (TFET). International Journal of Applied Engineering Research. 2016 April; 11(7): 4922–9.
- Choi WY, Lee WJ. Hetero-Gate-Dielectric tunneling Field Effect Transistors. IEEE Transactions on Electron Devices. 2010 Sep; 57(9): 2317–9.
- Choi WY, Park BG, Lee JD, Liu T-JK. Tunneling Field-Effect Transistors (TFETs) With Subthreshold Swing (SS) Less Than 60 mV/dec. IEEE Electron Device Letters. 2007 Aug; 28(8): 743–5.
- Wang PF, Hilsenbeck K, Nirschl, THM. Oswald, Stepper M, Weis D, Landsiedel S, Hansch W. Complementary tunneling transistor for low power application. Elsevier: Solid-State Electronics. 2004 Dec; 48(12): 2281–6. Crossref
- Nirschl Th, Wang PF, Hansch W, Landsiedel SD. The tunnelling field effect transistors (TFET) the temperature dependence, the simulation model, and its application. In Proceedings of the 2004 International Symposium on Circuits and Systems. 2004 May; 3: 713–6. Crossref
- Ionescu AM, Riel H. Tunnel field-effect transistors as energy-efficient electronic switches. 2011; 479: 329–37.
- Seabaugh AC, Zhang Q. Low-Voltage Tunnel Transistors for Beyond CMOS Logic. In Proceedings of IEEE. 2010 Dec; 98(2): 2095–110. Crossref
- Wang W, Wang PF, Zhang CM, Lin X, Liu XY, Sun QQ, Zhou, Zhang DW. Design of U-Shape Channel Tunnel FETs with SiGe Source Regions. 2014 Jan; 61(1): 193–7.
- Sant S, Schenk A. Methods to Enhance the Performance of InGaAs/InP Heterojunction Tunnel FETs. 2015 May; 63(5): 2169–75.
- Sahay S, Kumar MJ. Controlling the Drain Side Tunneling Width to Reduce Ambipolar Current in Tunnel FETs using Hetero-Dielectric BOX. 2015 Nov; 62911);:3882–6.
- Bhowmick B, Baishya S, Kar R. Length scaling of Hetero-gate dielectric SOI PNP TFET. 2011 Annual IEEE India Conference. 2011 Dec; 1–4. Crossref
- Aswathy M, Biju NM, Komaragiri R. Simulation Studies of a Tunnel Field Effect Transistor (TFET). In Proceedings of the 2012 International Conference on Advances in Computing and Communications (ICACC), Kerala, India. 2012 Aug; 138–41.
- Ashwin SR, Sreejith S, Sajeshkumar U. TCAD Design of Tunnel FET Structures and Extraction of Electrical Characteristics. International Journal of Science and Research (IJSR). 2015; 4(7):2447–51.
- Amrutha TP, Nesamani FPI, Prabha LV. Design of Si/Sige Heterojunction Line Tunnel Field Effect Transistor (TFET) with High-K Dielectric. ARPN Journal of Engineering and Applied Sciences. 2015; 10(4): 1879–82.
- Chen YN, Chen CJ, Fan ML, Hu VPH, Su P, Chuang CT. Impacts of Work Function Variation and Line-Edge Roughness on TFET and FinFET Devices and 32-Bit CLA Circuits. Journal of Low Power Electronics and Applications. 2015 May; 5: 101–15. Crossref